



Effects of preparation conditions on the electrochemical and morphological characteristics of $\text{Li}_4\text{Ti}_5\text{O}_{12}$ powders prepared by spray pyrolysis

Seo Hee Ju, Yun Chan Kang*

Department of Chemical Engineering, Konkuk University, 1 Hwayang-dong, Gwangjin-gu, Seoul 143-701, Republic of Korea

ARTICLE INFO

Article history:

Received 27 June 2008

Received in revised form 4 September 2008

Accepted 26 September 2008

Available online 10 October 2008

Keywords:

Lithium titanate

Anode materials

Spray pyrolysis

Lithium secondary battery

ABSTRACT

$\text{Li}_4\text{Ti}_5\text{O}_{12}$ anode powders were prepared by post-treatment of the precursor powders obtained by spray pyrolysis at various preparation conditions. The precursor powders had fine size, narrow size distribution, dense inner structure and homogeneous composition when the flow rate of the carrier gas and the preparation temperature were 10 l min^{-1} and 800°C . The spherical shapes of the precursor powders obtained at the optimum preparation conditions maintained after post-treatment at a temperature of 800°C . The mean sizes of the $\text{Li}_4\text{Ti}_5\text{O}_{12}$ powders were controlled by changing the concentrations of the spray solution. The initial discharge capacities and cycle properties of the $\text{Li}_4\text{Ti}_5\text{O}_{12}$ powders were strongly affected by the preparation temperatures of the precursor powders. The optimum preparation temperature of the precursor powders was 800°C when the flow rate of the carrier gas was 10 l min^{-1} . The discharge capacities and cycle properties of the $\text{Li}_4\text{Ti}_5\text{O}_{12}$ powders were not affected by flow rates of the carrier gas. The $\text{Li}_4\text{Ti}_5\text{O}_{12}$ powders had good cycle properties irrespective of the concentrations of the spray solution. However, the $\text{Li}_4\text{Ti}_5\text{O}_{12}$ powders obtained from the spray solutions with high concentration above 0.5 M had high discharge capacities than those obtained from the spray solutions with low concentration below 0.1 M .

© 2008 Elsevier B.V. All rights reserved.

1. Introduction

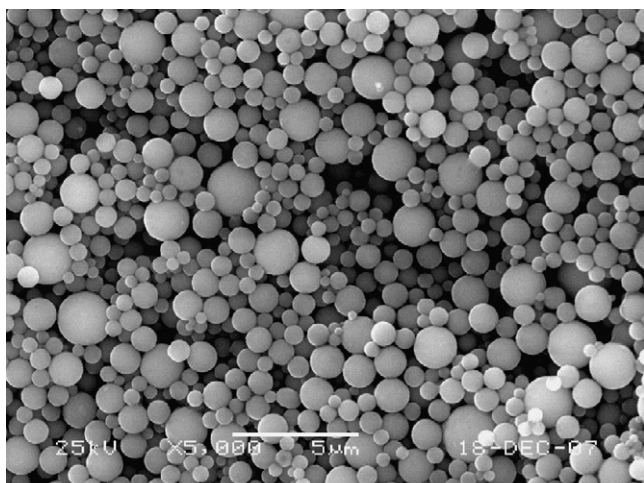
The spinel $\text{Li}_4\text{Ti}_5\text{O}_{12}$ is a so-called zero-strain insertion material as the anode material of lithium secondary batteries [1]. This material accommodates Li with a theoretical capacity of 175 mAh g^{-1} , and the actual discharge capacity is greater than 160 mAh g^{-1} [2]. $\text{Li}_4\text{Ti}_5\text{O}_{12}$ usually exhibits better electrochemical reversibility but the carbonaceous materials have the advantage to supply higher specific capacity values at lower potential, both items very important for an anode material. $\text{Li}_4\text{Ti}_5\text{O}_{12}$ powders could be synthesized by various conventional ceramic processes [3–7]. Therefore, this material is regarded as one of the promising anode materials. The characteristics of the anode materials were affected by the preparation processes of powders. Therefore, the various types of anode material were prepared by various solid state, liquid solution and gas-phase reaction methods. The morphological and electrochemical properties of the $\text{Li}_4\text{Ti}_5\text{O}_{12}$ powders prepared by solid state reaction and sol–gel methods were well known [4–7]. However, the characteristics of the $\text{Li}_4\text{Ti}_5\text{O}_{12}$ powders prepared by gas-phase reaction method were not well investigated.

Spray pyrolysis, which is one of the gas-phase reaction method, was applied to the preparation of various types of cathode and anode materials for lithium secondary batteries. In this study, spherical shape $\text{Li}_4\text{Ti}_5\text{O}_{12}$ anode powders were prepared by spray pyrolysis. The effects of preparation conditions on the crystal structure, the morphology, and the electrochemical performance of the $\text{Li}_4\text{Ti}_5\text{O}_{12}$ anode powders were investigated.

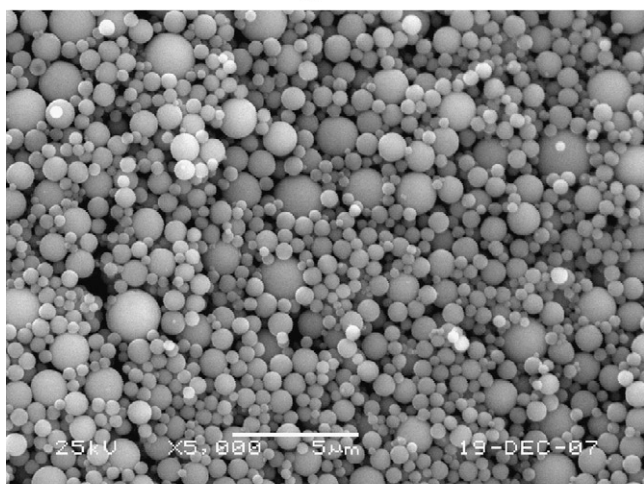
2. Experimental

The spray pyrolysis system consists of a droplet generator, a quartz reactor, and a powder collector. A 1.7-MHz ultrasonic spray generator with six vibrators was used to generate a large amount of droplets, which are carried into the high-temperature tubular reactor by a carrier gas. The droplets and powders evaporated, decomposed, and/or crystallized in the quartz reactor. The length and diameter of the quartz reactor were 1200 and 50 mm, respectively. The reactor temperatures were changed from 600°C to 1000°C . The flow rates of the air used as the carrier gas were changed from 10 to 40 l min^{-1} . The precursor solution was prepared by dissolving lithium nitrate (LiNO_3) and titanium(IV) tetraisopropoxide (TTIP, $\text{Ti}[\text{OCH}(\text{CH}_3)_2]_4$) in distilled water using small amount of nitric acid. The overall solution concentration of Li and Ti components were changed from 0.03 to 2 M . The as-prepared pow-

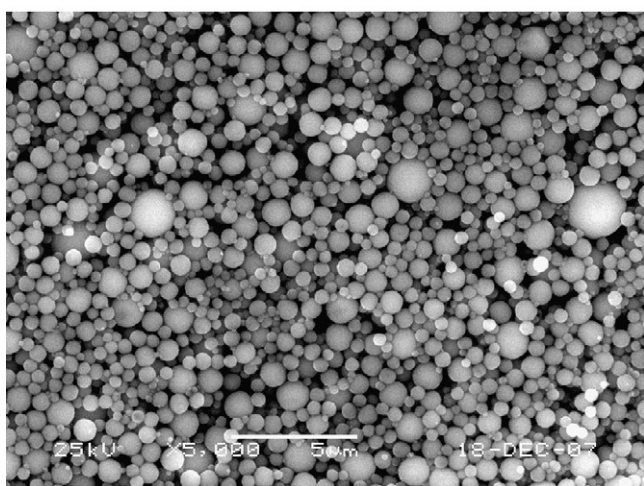
* Corresponding author. Tel.: +82 2 2049 6010; fax: +82 2 458 3504.
E-mail address: yckang@konkuk.ac.kr (Y.C. Kang).



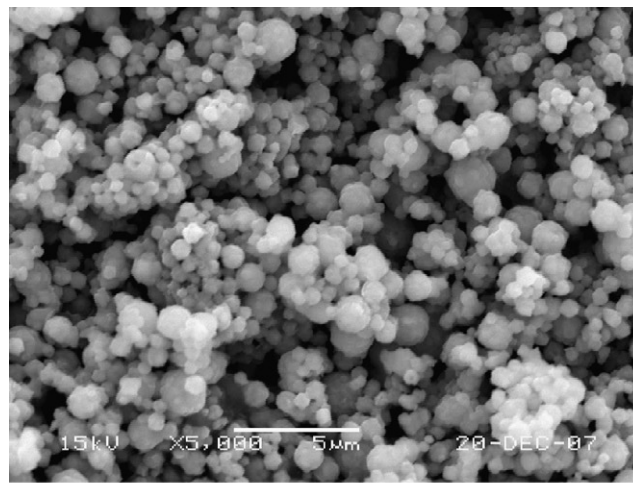
(a) P 600



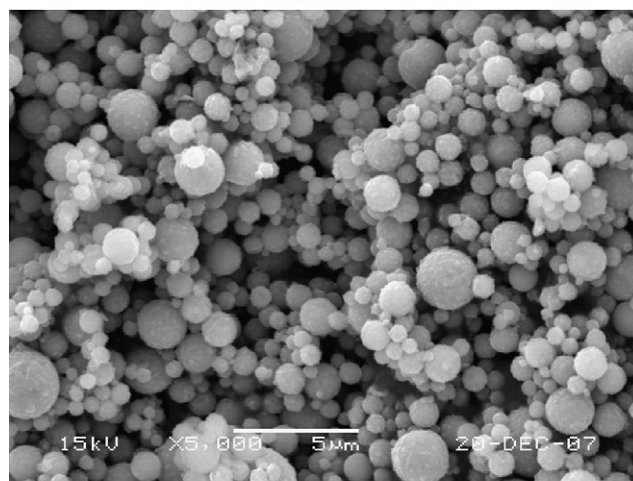
(b) P 800



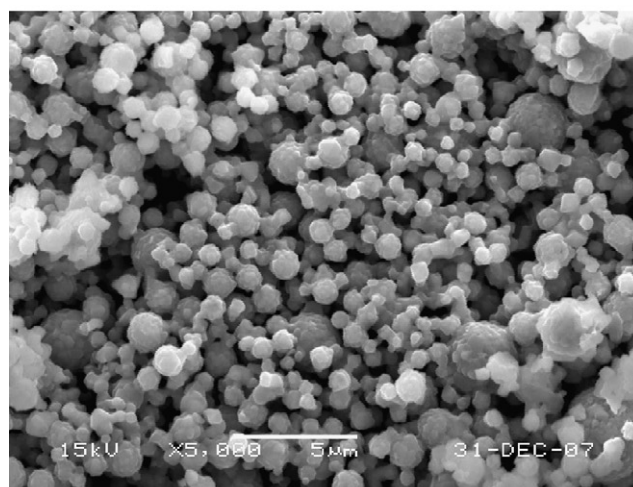
(c) P 1000



(a) P 600



(b) P 800



(c) P 1000

Fig. 1. SEM images of the precursor powders prepared at various temperatures.

Fig. 2. SEM images of the $\text{Li}_4\text{Ti}_5\text{O}_{12}$ powders obtained from the different preparation temperatures.

ders obtained by spray pyrolysis were post-treated at a temperature of 800 °C for 12 h in air atmosphere.

The crystal structures of the as-prepared and post-treated powders were investigated using X-ray diffractometry (XRD, RIGAKU DMAX-33) using Cu K α radiation ($\lambda = 1.5418 \times 10^{-10}$ m). The morphological characteristics of the powders were investigated using

scanning electron microscopy (SEM, JEOL JSM-6060). Surface areas and pore volumes of the powders were measured by Brunauer-Emmett-Teller (BET) method using N₂ as adsorbate gas. The charge/discharge capacities of the prepared $\text{Li}_4\text{Ti}_5\text{O}_{12}$ anode materials were measured. The anode electrode was made of 12 mg

of $\text{Li}_4\text{Ti}_5\text{O}_{12}$ compounds mixed with 4 mg of a conductive binder (3.2 mg of teflonized acetylene black and 0.8 mg of graphite). The lithium metal and polypropylene film were used as the counter electrode and the separator, respectively. The electrolyte (TECHNO Semichem. Co.) was 1 M LiPF_6 in a 1:1 mixture by volume of EC/DMC. The entire cell was assembled in a glove box under an argon atmosphere. The charge/discharge characteristics of the samples were measured through cycling in the 0.5–2.5 V potential range at variety current densities.

3. Results and discussion

The characteristics of the $\text{Li}_4\text{Ti}_5\text{O}_{12}$ powders prepared by spray pyrolysis were affected by the preparation conditions such as preparation temperature and residence time of powders inside the hot wall reactor. Fig. 1 shows the SEM images of the precursor powders obtained by spray pyrolysis at various preparation temperatures with constant flow rate of carrier gas as 10 l min^{-1} . The concentration of the spray solution was 0.5 M. The precursor powders had spherical morphologies irrespective of the preparation temperatures. However, the mean sizes of the precursor powders measured from the SEM images decreased with increasing the preparation temperatures. The mean sizes of the precursor

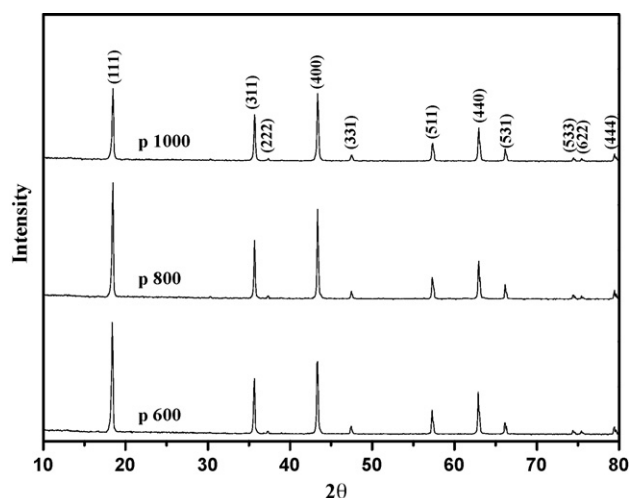


Fig. 3. XRD patterns of the $\text{Li}_4\text{Ti}_5\text{O}_{12}$ powders obtained from the different preparation temperatures.

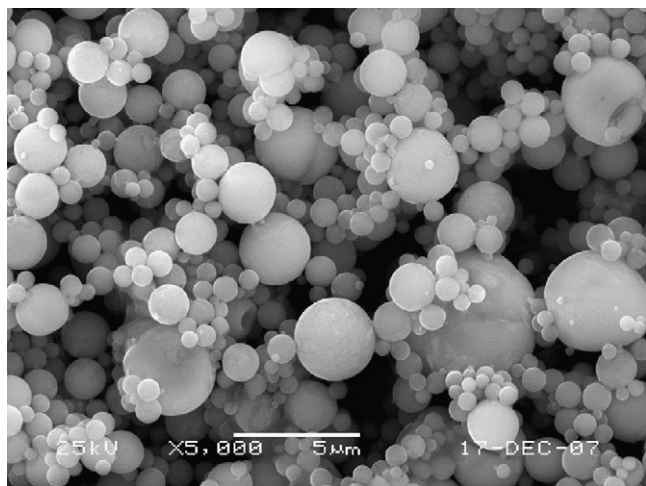


Fig. 4. SEM image of the precursor powders obtained at high flow rate of carrier gas.

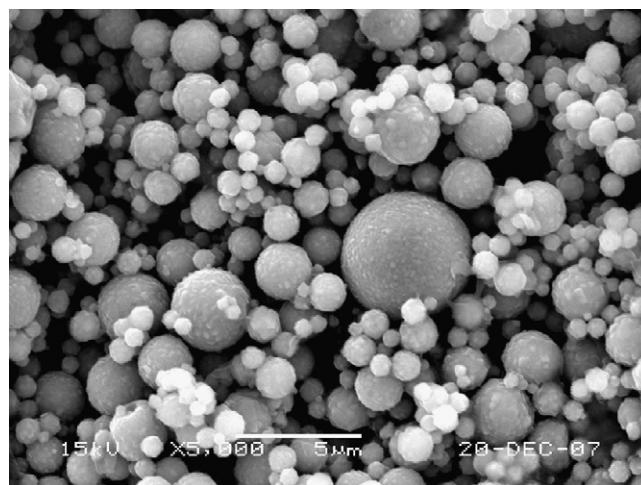
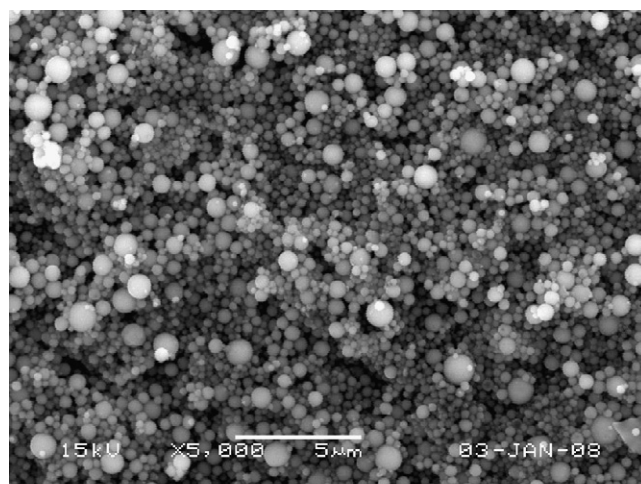
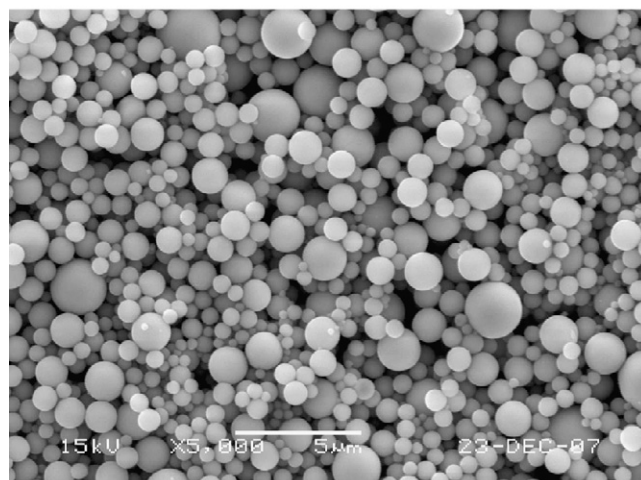


Fig. 5. SEM image of the $\text{Li}_4\text{Ti}_5\text{O}_{12}$ powders obtained at high flow rate of carrier gas.



(a) 0.03 M



(b) 2 M

Fig. 6. SEM images of the precursor powders obtained from the spray solutions with different concentrations.

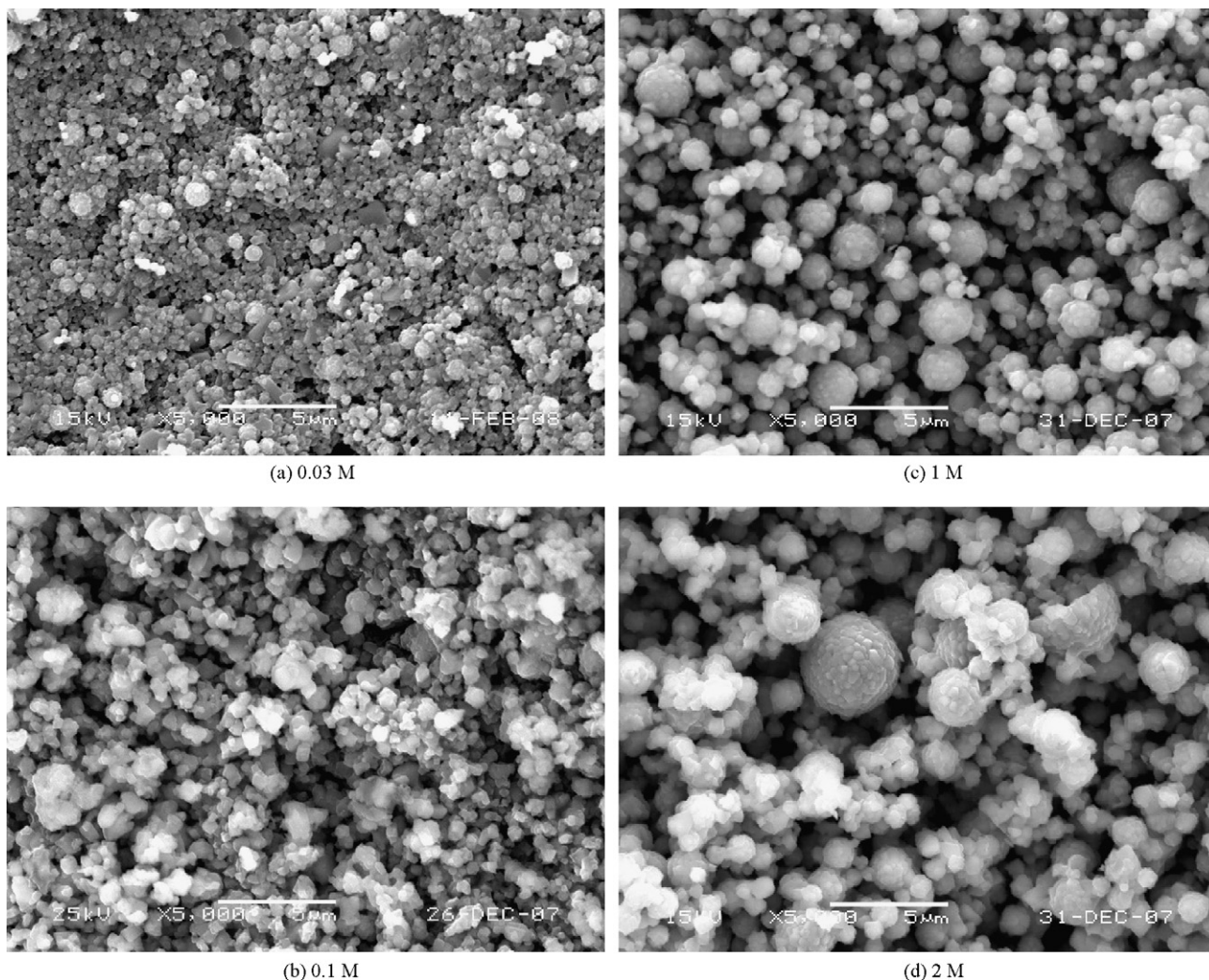


Fig. 7. SEM images of the $\text{Li}_4\text{Ti}_5\text{O}_{12}$ powders obtained from the spray solutions with different concentrations.

powders prepared at temperatures of 600 and 1000 °C were 1.2 and 0.7 μm . The geometric standard deviations of the precursor powders prepared at temperatures of 600 and 1000 °C were 1.7 and 1.5. The different morphologies of the precursor powders prepared at various preparation temperatures changed the mean sizes and size distributions. The precursor powders prepared at a temperature of 600 °C had more hollow structure than those prepared at a temperature of 1000 °C. The precursor powders did not have crystalline $\text{Li}_4\text{Ti}_5\text{O}_{12}$ phase because of short residence time of the powders inside the hot wall reactor. Therefore, the precursor powders obtained by spray pyrolysis at various preparation temperatures were post-treated at a temperature of 800 °C in a box furnace. Fig. 2 shows the SEM images of the post-treated $\text{Li}_4\text{Ti}_5\text{O}_{12}$ powders. The spherical shape of the precursor powders maintained after post-treatment irrespective of the preparation temperatures of the precursor powders. The $\text{Li}_4\text{Ti}_5\text{O}_{12}$ powders obtained from the precursor powders as shown in Fig. 1(a) and (b) had slight aggregation characteristics. On the other hand, aggregation between the $\text{Li}_4\text{Ti}_5\text{O}_{12}$ powders as shown in Fig. 2(c) observed. Fig. 3 shows the XRD patterns of the post-treated $\text{Li}_4\text{Ti}_5\text{O}_{12}$ powders. The post-treated powders had the single phase of spinel $\text{Li}_4\text{Ti}_5\text{O}_{12}$ phase without impurity peaks irrespective of the preparation temperatures of the precursor powders. All the diffraction peaks can be indexed based on a face-centered cubic spinel struc-

ture with an $\text{Fd}3\text{m}$ space group [8]. The mean crystallite sizes of the $\text{Li}_4\text{Ti}_5\text{O}_{12}$ powders as shown in Fig. 2(a)–(c) measured from Fig. 3 were 47, 44 and 39 nm. The preparation temperature affected the morphologies and mean sizes of the precursor powders as shown in Fig. 1. Therefore, the morphologies and mean crystallite sizes of the post-treated $\text{Li}_4\text{Ti}_5\text{O}_{12}$ powders were affected by the preparation temperatures of the precursor powders. The post-treated $\text{Li}_4\text{Ti}_5\text{O}_{12}$ powders had low pore volumes inside the powders irrespective of the preparation temperatures of the precursor powders. Therefore, the post-treated $\text{Li}_4\text{Ti}_5\text{O}_{12}$ powders as shown in Fig. 2(a)–(c) had low BET surface areas as 1.72, 2.36 and 1.98 $\text{m}^2 \text{g}^{-1}$.

In order to investigate the effect of residence time of the powders inside the hot wall reactor on the properties of $\text{Li}_4\text{Ti}_5\text{O}_{12}$ powders, the precursor powders were prepared at various flow rates of the carrier gas. Fig. 4 shows the SEM image of the precursor powders prepared at high flow rate of the carrier gas. The preparation temperature of the precursor powders was 800 °C. The concentration of the spray solution was 0.5 M. The precursor powders had spherical shapes irrespective of the high flow rate of the carrier gas. However, the hollowness of the precursor powders increased with increasing the flow rate of the carrier gas. Therefore, the precursor powders (Fig. 1(b)) prepared at a low flow rate of the carrier gas as 10 l min^{-1} had finer size than those prepared at high flow rate of the carrier gas

as 301 min^{-1} . The high drying and decomposition rates of droplet or powders increased the hollowness of the precursor powders when the flow rate of the carrier gas was too high. The residence time of droplet/powder inside the hot wall reactor were changed from 2.6 to 0.7 s when the flow rate of the carrier gas increased from 10 to 301 min^{-1} . Fig. 5 shows the SEM image of the $\text{Li}_4\text{Ti}_5\text{O}_{12}$ powders post-treated at a temperature of 800°C . In Fig. 2(b) and Fig. 5, the $\text{Li}_4\text{Ti}_5\text{O}_{12}$ powders had spherical shape and non-aggregation characteristics irrespective of the flow rate of the carrier gas. The mean size of the $\text{Li}_4\text{Ti}_5\text{O}_{12}$ powders as shown in Fig. 5 was $1.8 \mu\text{m}$. However, the mean size of the $\text{Li}_4\text{Ti}_5\text{O}_{12}$ powders as shown in Fig. 2(b) was $0.98 \mu\text{m}$.

Fig. 6 shows the SEM images of the precursor powders prepared from the spray solutions with various concentrations. The preparation temperature and the flow rate of the carrier gas were 800°C and 101 min^{-1} . The $\text{Li}_4\text{Ti}_5\text{O}_{12}$ powders had spherical shapes and non-aggregation characteristics irrespective of the spray solution concentrations. However, the mean size of the precursor powders increased with increasing the solution concentrations of the spray solution. The mean sizes of the precursor powders increased from 0.52 to $1.2 \mu\text{m}$ when the concentration of the spray solution was increased from 0.03 to 2 M . Fig. 7 shows the SEM images of the post-treated $\text{Li}_4\text{Ti}_5\text{O}_{12}$ powders. The spherical shapes of the precursor powders obtained from the spray solutions with low concentrations below 0.1 M disappeared after post-treatment because of low thermal stability of the fine-sized powders. However, spherical shapes of the precursor powders obtained from the spray solutions with high concentrations above 0.5 M maintained after post-treatment.

The initial charge/discharge capacities and cycle properties of the post-treated $\text{Li}_4\text{Ti}_5\text{O}_{12}$ powders prepared at various conditions were shown in Figs. 8–11. Figs. 8 and 9 show the effect of the preparation temperatures of the precursor powders on the initial charge/discharge capacities and cycle properties of the $\text{Li}_4\text{Ti}_5\text{O}_{12}$ powders. As can be seen in Fig. 8, all the profiles exhibited extremely flat operating voltage at about 1.5 V (versus Li), which is consistent with the results of the previous study [7]. During the subsequent charge process, a very flat charge curve at around 1.6 V (versus Li) can be observed and the discharge and charge voltage are close. This suggests a two-phase reaction based on the $\text{Ti}^{4+}/\text{Ti}^{3+}$ redox couple as described in the previous study [2]. The initial charge/discharge capacities of the $\text{Li}_4\text{Ti}_5\text{O}_{12}$ powders were affected by the preparation temperatures of the precursor powders. As shown in Fig. 8, the initial discharge capacities of the $\text{Li}_4\text{Ti}_5\text{O}_{12}$ powders as shown in Fig. 2(b) and (c) were high as 171 and 172 mAh g^{-1} . On the other hand, the $\text{Li}_4\text{Ti}_5\text{O}_{12}$ powders as shown in Fig. 2(a) had low discharge capacity of 126 mAh g^{-1} . The discharge capacity of the $\text{Li}_4\text{Ti}_5\text{O}_{12}$ powders as shown in Fig. 2(b) dropped from 171 to 168 mAh g^{-1} by the 50th cycle. The $\text{Li}_4\text{Ti}_5\text{O}_{12}$ powders as shown in Fig. 2(a) had also good retention capacity value on cycling. On the other hand, the $\text{Li}_4\text{Ti}_5\text{O}_{12}$ powders as shown in Fig. 2(c) had poor cycle properties. The discharge capacity of the $\text{Li}_4\text{Ti}_5\text{O}_{12}$ powders as shown in Fig. 2(c) dropped from 172 to 129 mAh g^{-1} by the 50th cycle.

Fig. 10 shows the effect of the flow rate of the carrier gas on the cycle properties of the $\text{Li}_4\text{Ti}_5\text{O}_{12}$ powders. The $\text{Li}_4\text{Ti}_5\text{O}_{12}$ powders had similar initial discharge capacities and cycle properties irrespective of the flow rate of the carrier gas. The flow rate of the carrier gas did not change the composition of the precursor powders. Therefore, the discharge capacities and cycle properties of the $\text{Li}_4\text{Ti}_5\text{O}_{12}$ powders were not affected by the flow rates of the carrier gas. Fig. 11 shows the effect of the concentrations of the spray solution on the cycle properties of the $\text{Li}_4\text{Ti}_5\text{O}_{12}$ powders. The $\text{Li}_4\text{Ti}_5\text{O}_{12}$ powders obtained from the spray solutions with high concentrations above 0.5 M had good cycle properties. After 70 cycles, the

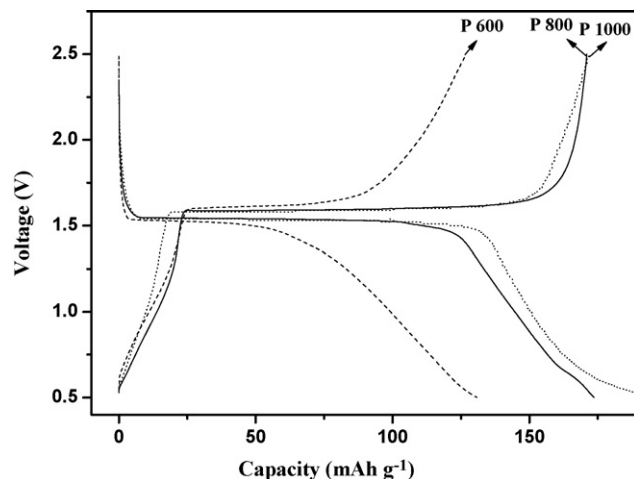


Fig. 8. Initial charge/discharge curves of the $\text{Li}_4\text{Ti}_5\text{O}_{12}$ powders obtained at different preparation temperatures.

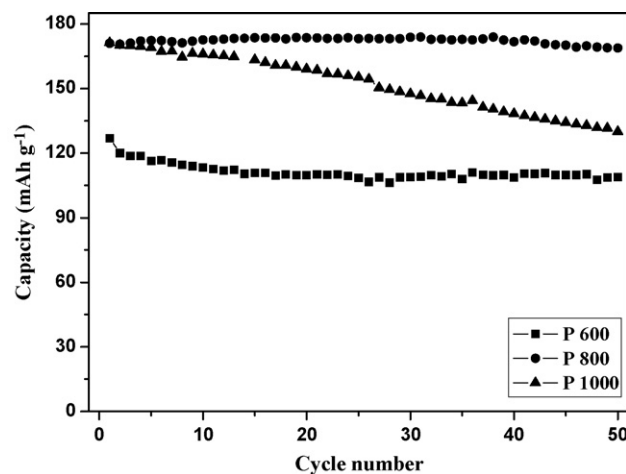


Fig. 9. Cycle properties of the $\text{Li}_4\text{Ti}_5\text{O}_{12}$ powders obtained at different preparation temperatures.

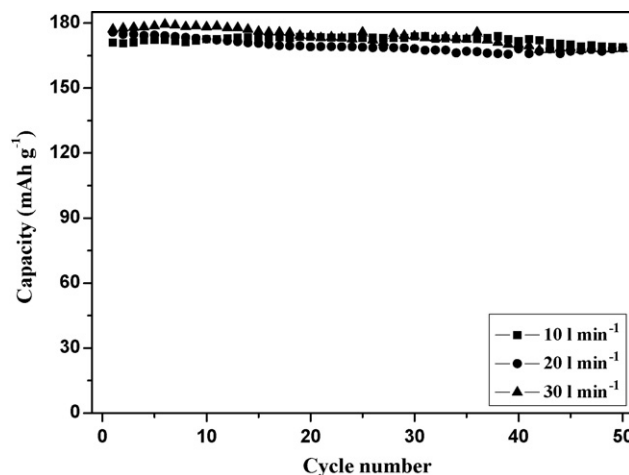


Fig. 10. Cycle properties of the $\text{Li}_4\text{Ti}_5\text{O}_{12}$ powders obtained at different flow rate of the carrier gas.

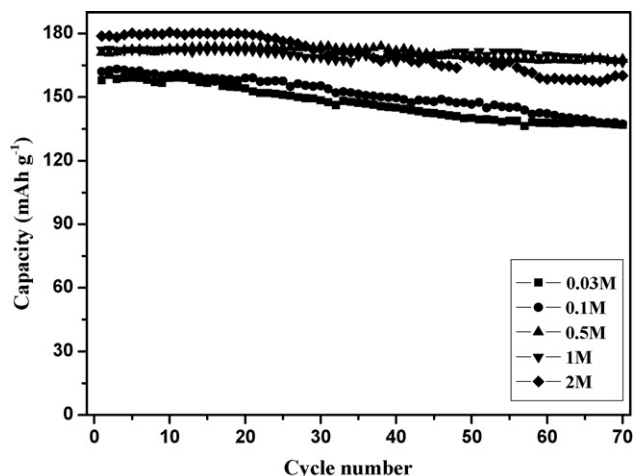


Fig. 11. Cycle properties of the $\text{Li}_4\text{Ti}_5\text{O}_{12}$ powders obtained from the spray solutions with different concentration.

discharge capacities of the $\text{Li}_4\text{Ti}_5\text{O}_{12}$ powders as shown in Fig. 2(b), Fig. 7(c) and (d) were 98, 97, and 90% of the initial discharge capacities. On the other hand, the $\text{Li}_4\text{Ti}_5\text{O}_{12}$ powders obtained from the spray solutions with low concentrations below 0.1 M had poor cycle properties. After 70 cycles, the discharge capacities of the $\text{Li}_4\text{Ti}_5\text{O}_{12}$

powders as shown in Fig. 7(a) and (b) were 85 and 86% of the initial discharge capacities.

4. Conclusion

$\text{Li}_4\text{Ti}_5\text{O}_{12}$ powders as anode material for lithium secondary battery were prepared by spray pyrolysis. The morphologies and charge/discharge capacities of the $\text{Li}_4\text{Ti}_5\text{O}_{12}$ anode powders obtained by spray pyrolysis at various preparation conditions were investigated. The post-treated powders obtained at the optimum preparation conditions had spherical shape with spinel $\text{Li}_4\text{Ti}_5\text{O}_{12}$ phase. The initial discharge capacities and cycle properties of the $\text{Li}_4\text{Ti}_5\text{O}_{12}$ powders were strongly affected by preparation conditions of the precursor powders. The $\text{Li}_4\text{Ti}_5\text{O}_{12}$ anode powders prepared at the optimum conditions had high discharge capacities larger than 171 mAh g^{-1} and good cycle properties.

References

- [1] T. Ohzuku, A. Ueda, N. Yamamoto, J. Electrochem. Soc. 142 (5) (1995) 1431.
- [2] J. Wolfenstine, S. Campos, D. Foster, J. Power Sources 109 (2002) 230.
- [3] J. Gao, C. Jiang, J. Ying, C. Wan, J. Power Sources 155 (2006) 364.
- [4] P. Birke, F. Salam, S. Döring, W. Weppner, Solid State Ionics 118 (1999) 149.
- [5] Y.H. Rho, K. Kanamura, M. Fujisaki, J. Hamagami, S. Suda, T. Umegaki, J. Solid State Ionics 151 (2002) 151.
- [6] S. Bach, J.P. Pereira-Ramos, N. Baffier, J. Power Sources 273 (1999) 81.
- [7] G.X. Wang, D.H. Bradhurst, S.X. Dou, H.K. Liu, J. Power Sources 83 (1999) 156.
- [8] A. Deschanvers, B. Raveau, Z. Sekkal, Mater. Res. Bull. 6 (1971) 699.